

# DOP: Deep Optimistic Planning with Approximate Value Function Evaluation

Francesco Riccio  
Sapienza University of Rome,  
Department of Computer, Control  
and Management Engineering  
Via Ariosto 25, Rome, Italy  
riccio@diag.uniroma1.it

Roberto Capobianco  
Sapienza University of Rome,  
Department of Computer, Control  
and Management Engineering  
Via Ariosto 25, Rome, Italy  
capobianco@diag.uniroma1.it

Daniele Nardi  
Sapienza University of Rome,  
Department of Computer, Control  
and Management Engineering  
Via Ariosto 25, Rome, Italy  
nardi@diag.uniroma1.it

## ABSTRACT

Research on reinforcement learning has demonstrated promising results in manifold applications and domains. Still, efficiently learning effective robot behaviors is very difficult, due to unstructured scenarios, high uncertainties, and large state dimensionality (e.g. multi-agent systems or hyper-redundant robots). To alleviate this problem, we present DOP, a deep model-based reinforcement learning algorithm, which exploits action values to both (1) guide the exploration of the state space and (2) plan effective policies. Specifically, we exploit deep neural networks to learn  $Q$ -functions that are used to attack the curse of dimensionality during a Monte-Carlo tree search. Our algorithm, in fact, constructs upper confidence bounds on the learned value function to select actions optimistically. We implement and evaluate DOP on different scenarios: (1) a cooperative navigation problem, (2) a fetching task for a 7-DOF KUKA robot, and (3) a human-robot handover with a humanoid robot (both in simulation and real). The obtained results show the effectiveness of DOP in the chosen applications, where action values drive the exploration and reduce the computational demand of the planning process while achieving good performance.

## KEYWORDS

Robot Learning; Reinforcement Learning; Deep Reinforcement Learning; Planning

### ACM Reference Format:

Francesco Riccio, Roberto Capobianco, and Daniele Nardi. 2018. DOP: Deep Optimistic Planning with Approximate Value Function Evaluation. In *to appear as an extended abstract paper in the Proc. of the 17th International Conference on Autonomous Agents and Multiagent Systems (AAMAS 2018)*, Stockholm, Sweden, July 10–15, 2018, IFAAMAS, 7 pages.

## 1 INTRODUCTION

Action planning in robotics is a complex task due to unpredictabilities of the physical world, uncertainties in the observations, and rapid explosions of the state dimensionality. For example, hyper-redundant manipulators are typically affected by the curse of dimensionality problem when planning in large state spaces. Similarly, in multi-robot collaborative tasks, each robot has to account for both the state of the environment and other robots' states. Due to the curse of dimensionality, generalization and policy generation are

*to appear as an extended abstract paper in the Proc. of the 17th International Conference on Autonomous Agents and Multiagent Systems (AAMAS 2018)*, M. Dastani, G. Sukthankar, E. André, S. Koenig (eds.), July 10–15, 2018, Stockholm, Sweden. © 2018 International Foundation for Autonomous Agents and Multiagent Systems (www.ifaamas.org). All rights reserved.

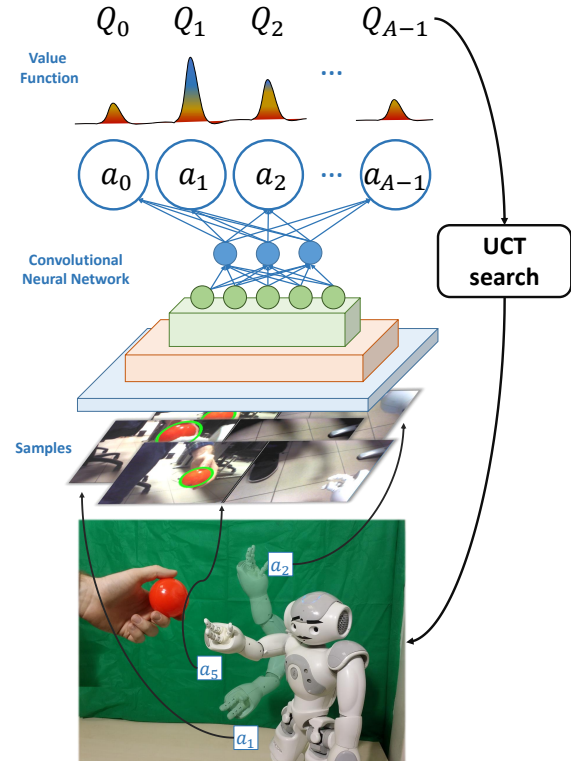


**Figure 1: Overview of DOP. Action values are learned with a deep convolutional neural network over observations collected from robot experience. These  $Q$ -values are then explicitly used at planning time to prune actions evaluated during a Monte-Carlo tree search.**

time consuming and resource intensive. While deep learning approaches led to improved generalization capabilities and major successes in reinforcement learning [9–11] and robot planning [7, 8], most techniques require huge amounts of data collected through agent's experience. In robotics, this is often achieved by spawning multiple simulations [15] in parallel to feed a single neural network. During simulation, however, the robot explores its huge search space, with little or no prior knowledge. While encoding prior information in robot behaviors is often desirable, this is difficult when using neural networks and it is mostly achieved through imitation learning [2, 20] with little performance guarantees. To overcome

this issue, decision theoretical planning techniques, such as Monte-Carlo tree search [1], have been applied in literature. Unfortunately, these methods fail in generalizing and show limitations in relating similar states [18] (i.e. nodes of the search tree).

As in prior work [12], we attack the generalization problem in policy generation by enhancing the Upper Confidence Tree (UCT) algorithm [6] – a variant of Monte-Carlo tree search – with an external action-value function approximator, that selects admissible actions and consequently drives the node-expansion phase during episode simulation. In particular, in this paper, we extend the algorithm in [12] to use a more powerful representation, based on deep learning, that enables better generalization and supports higher dimensional problems. In fact, DOP (Deep Optimistic Planning), is based on  $Q$ -learning and allows agents to plan complex behaviors in scenarios characterized by discrete action spaces and large state spaces. As shown in Figure 1, to model action values, we use a convolutional neural network (CNN) that is iteratively refined by aggregating [14] samples collected at every timestep. Specifically, DOP generates action policies by running a Monte Carlo tree search [22] and incrementally collecting new samples that are used to improve a deep  $Q$ -network approximating action values.

We aim at demonstrating that DOP can efficiently be used to generalize policies and restrict the search space to support learning in high-dimensional state spaces. To this end, we address applications that involve multi and hyper-redundant robots by evaluating DOP over three complex scenarios: a cooperative navigation task of 3 Pioneer robots in a simple environment, a fetching task with a 7-DOF KUKA arm, and an handover task with a humanoid NAO robot. The experimental evaluation shows the effectiveness of using deep learning to represent action values that are exploited in the search process, resulting in improved generalization capabilities of the planning algorithm – that make it suitable also for multi-agent domains. Our main contributions consist in (1) an extension of prior work [12] to use deep learning and improve both the focused exploration and generalization capabilities, and (2) an extended experimental evaluation of the representation and the algorithm, that shows the usability of DOP in complex high-dimensional and multi-robot domains.

The remainder of the paper is organized as follows. Section 2 reports recent research on (deep) reinforcement learning and planning, and Section 3 describes the DOP representation and algorithm. Finally, Section 4 describes our experimental setup, as well as the obtained results, and Section 5 discusses final remarks, limitations and future directions.

## 2 RELATED WORK

Recent trends in reinforcement learning have shown improved generalization capabilities, by exploiting deep learning techniques. For example, Mnih et al. [11] use a deep  $Q$ -network to learn directly from high-dimensional visual sensory inputs on Atari 2600 games. Silver et al. [16, 17] use deep value networks and policy networks to respectively evaluate board positions and select moves to achieve superhuman performance in Go. In [10], instead, the authors execute multiple agents in parallel, on several instances of the same environment, to learn a variety of tasks using actor-critic

with asynchronous gradient descent. Similar advancements have been shown in the robotics domain. For instance, Levine et al. [7] represent policies through deep convolutional neural networks, and train them using a partially observed guided policy search method on real-world manipulation tasks. Moreover, Rusu et al. [15] use deep learning in simulation, and propose progressive networks to bridge the reality gap and transfer learned policies from simulation to the real world. Unfortunately, planning and learning with deep networks is computationally demanding (i.e., requires a huge number of heavy simulations). For this reason, Weber et al. [21] introduce I2As to exploit outcome of virtual policy executions, in the Sokoban domain, learned with a deep network.

During simulation, the robot uninformedly explores its search space, and attempts to find an optimal policy. To facilitate this task, several approaches initialize robot policies with reasonable behaviors collected from human experts (e.g., through the aid of expert demonstrations [11, 19]). For example, in [20] the authors rely on a Deep Deterministic Policy Gradient approach to exploit expert demonstration in object insertion tasks. These methods, however, generally require a considerable number of training examples, and are not easily applicable to complex domains, such as multi-agent scenarios and highly redundant robots. While traditional decision theoretic planning methods, such as Monte-Carlo tree search [1, 6], enable easier injection of prior knowledge in generated behaviors, they do not provide sufficient generalization capabilities, that are required in common robotics problems, where large portions of the state space are rarely or never explored.

In this paper, we address generalization at learning time by introducing DOP, an iterative algorithm for policy generation that makes use of deep  $Q$ -networks to drive a focused exploration. DOP relies on previous work [12] and extends it with a different representation to obtain improved generalization capabilities over higher dimensional problems. In particular, we approximate the  $Q$  function using  $Q$ -learning with a deep convolutional neural network. Similar to  $Q$ -CP [12] and TD-search [18], we aim at reducing the variance of value estimates during the search procedure by means of temporal difference learning. However, as in [12], DOP extends TD-search by constructing upper confidence bounds on the value function, and by selecting optimistically with respect to those, instead of performing  $\epsilon$ -greedy exploration. Thanks to the generalization capabilities of deep networks, DOP improves over  $Q$ -CP both in terms of policy and exploration. Our representation, in fact, not only enables the algorithm to explore more informative portions of the search space [3, 4], but also is able to generalize better among them with positive effects on the overall policy and search space expansion.

## 3 DOP

We describe DOP by adopting the standard Markov Decision Process (MDP) notation, in which the decision-making problem is represented as a tuple

$$MDP = (S, A, \mathcal{T}, R, \gamma),$$

where  $S$  is the set of states of the environment,  $A$  represents the set of discrete actions available to the agent,  $\mathcal{T} : S \times A \times S \rightarrow [0, 1]$  is the stochastic transition function that models the probabilities of transitioning from state  $s \in S$  to  $s' \in S$  when an action is executed,  $R : S \times A \rightarrow \mathbb{R}$  is the reward function. In this setting, actions

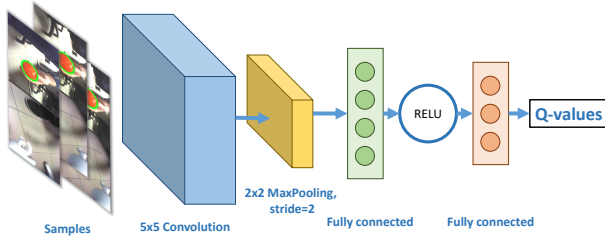


**Figure 2: Deep convolutional neural network adopted in DOP. The network is implemented within the Caffe2 environment.**

are chosen according to a policy  $\pi(a|s)$  (or more simply  $\pi(s)$ ), that maps states to actions. Given an MDP, the goal of the agent consists in finding a policy  $\pi(s)$  that maximizes its future reward with a discount factor  $\gamma \in [0, 1)$ .

Under this framework, DOP builds on [12] and iteratively evolves by (1) running a Monte-Carlo tree search, where admissible actions are selected through  $Q$ -value estimates learned through a deep neural network and (2) incrementally collecting new samples that are used to improve  $Q$ -value estimates. In this section, we first describe our representation for the  $Q$  function; then, we present an explanation of the algorithm.

### 3.1 Representation

As in previous literature [10, 11], we choose to change the representation adopted in [12] and approximate the action values using a deep neural network. In particular, we adopt a deep neural network (implemented in Caffe2<sup>1</sup>), composed by a convolutional layer, followed by a max pooling operator and two fully connected layers, one with ReLU activations, the other linear. The input of the network is an image capturing the state of the environment, and its output is the  $Q$  value for each action. In our work, we always assume one single frame to be sufficient to fully represent the state  $s$  at each timestep, and we store in our dataset transitions  $x = (s_t, a_t, s_{t+1}, r_{t+1})$ .

Differently from DQN, we do not explicitly make use of an experience replay buffer, and we replace it with a data aggregation [14] procedure, where all the transitions are iteratively collected, aggregated and used at training time. Specifically, at each iteration  $i$  of DOP we collect a dataset  $D^i = \{x\}$  of transitions experienced by the agent, and we aggregate it into  $D^{0:i} = \{\cup D^d | d = 0 \dots i\}$ , that is used for learning. In practice, this results in a very similar mechanism that enables data decorrelation and facilitates learning. In fact, the network is always re-trained using mini-batches of samples randomly selected within  $D^{0:i}$ , until the dataset is exhaustively used. Hence, each mini-batch is less affected by the non-i.i.d structure of the dataset, and this procedure closely resembles the more standard replay mechanism.

The aggregated dataset is finally used to minimize the  $\ell_2$ -loss:

$$\ell_2(r_{t+1} + \gamma \max_{a'} Q_\theta(s_{t+1}, a'), Q_\theta(s_t, a_t)), \quad (1)$$

<sup>1</sup><https://caffe2.ai>

where  $\theta$  are the current parameters of the network. The optimization is performed using an Adam [5] optimizer with a learning rate  $\alpha$  selected according to the task.

### 3.2 Algorithm

DOP builds on  $Q$ -CP [12], which is an iterative algorithm that, at each iteration  $i$ , (1) generates a new policy  $\pi_i$  which improves  $\pi_{i-1}$  and (2) learns action values that are used at planning time to reduce the search space. In this section, we briefly describe the algorithm by adapting its discussion to the representation adopted in DOP. Specifically, at every iteration the agent executes a UCT search, where admissible actions are selected through  $Q$  value estimates, and incrementally collects new samples that are used to improve  $Q$  value estimates as described in previous section.

More in detail (see Algorithm 1), DOP takes as input an initial policy  $\pi^0$  and, at each iteration  $i = 1 \dots I$ , evolves as follows:

- (1) the agent follows its policy  $\pi^{i-1}$  for  $T$  timesteps, generating a set of  $T$  states  $\{s_t\}$ ;
- (2) for each generated state  $s_t$ , the agent runs a modified UCT search [6] with depth  $H$ . Specifically, at each  $h = 1 \dots H$ , the search algorithm
  - (a) evaluates a subset of “admissible” actions  $\tilde{A} \subseteq A$  in  $s_{t+(h-1)}$ , that are determined according to  $Q_\theta(s_{t+(h-1)}, a)$ . In particular, differently from vanilla UCT, we only allow actions  $a$  such that

$$Q_\theta(s_{t+(h-1)}, a) \geq \lambda \max_a Q_\theta(s_{t+(h-1)}, a) + \epsilon_{\tilde{A}} \quad (2)$$

where  $\lambda$  is typically initialized to 0.5 and increases with the number of iterations  $i$ . Through  $\epsilon_{\tilde{A}}$ , a certain amount of exploration is guaranteed;

- (b) selects and executes the best action  $a_h^* \in \tilde{A}$  according to

$$e = C \cdot \sqrt{\frac{\log(\sum_a \eta(s_{t+(h-1)}, a))}{\eta(s_{t+(h-1)}, a)}} \quad (3)$$

$$a_h^* = \arg \max_a Q_\theta(s_{t+(h-1)}, a) + e,$$

where  $C$  is a constant that multiplies and controls the exploration term  $e$ , and  $\eta(s_{t+(h-1)}, a)$  is the number of occurrences of  $a$  in  $s_{t+(h-1)}$ . To use DOP on robotic applications with images as state representations, we define a comparison operator that introduces a discretization by computing whether the difference of two states is smaller than a given threshold  $\xi$ ;

- (c) runs  $M$  simulations (or roll-outs), by executing an  $\epsilon$ -greedy policy based on  $\pi^{i-1}$  until a terminal state is reached. DOP uses UCT as an expert and collects, a dataset  $D^i$  of  $H$  transitions experienced in simulation.
- (3)  $D^i$  is aggregated into  $D^{0:i} = D^i \cup D^{0:i-1}$  [13, 14], and the dataset is used to perform updates of the  $Q$ -network, as illustrated in previous section.
- (4) once  $Q_\theta$  is updated, the policy is generated as to maximize the action values:  $\pi^i(s) = \arg \max_a Q_\theta(s, a)$ .

## 4 EXPERIMENTAL EVALUATION

One of the main contributions of this paper consists in an extended experimental evaluation of the representation and the algorithm,

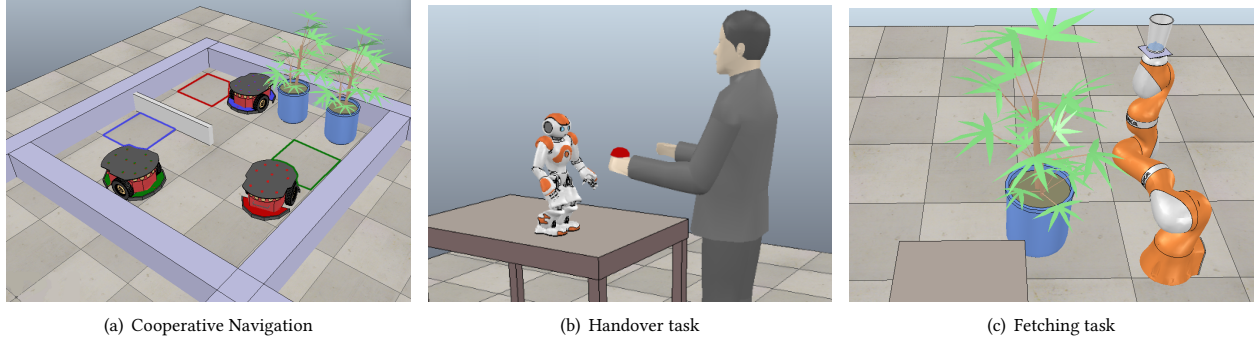


Figure 3: We evaluate DOP on three scenarios with different robots. Left: cooperative navigation scenario; middle: handover with the NAO robot; right: the fetching task with the 7-DOF KUKA arm.

---

**Algorithm 1:** DOP

---

**Data:**  $I$  the number of iterations;  $\Delta$  initial state distribution;  $H$  UCT horizon;  $T$  policy execution timesteps,  $\lambda_0$  initial max.  $Q$  threshold multiplier for admissible actions,  $\epsilon_{\hat{A}}$  probability for random admissible actions,  $\alpha$  learning rate,  $\gamma$  discount factor.

**Input:**  $\pi^0$  initial policy of the agent.

**Output:**  $\pi^I$  policy learned after  $I$  iterations.

**begin**

**for**  $i = 1$  **to**  $I$  **do**

$s_0 \leftarrow$  random state from  $\Delta$ .

**for**  $t = 1$  **to**  $T$  **do**

1)        Get state  $s_t$  by executing  $\pi^{i-1}(s_{t-1})$ .

2)         $D^i \leftarrow \text{UCT}_{\text{DOP}}(s_t, \lambda_0, \epsilon_{\hat{A}})$ .

3)         $D^{0:i} \leftarrow D^i \cup D^{0:i-1}$ .

$Q_{\theta}.\text{UPDATE}(D^{0:i}, \alpha, \gamma)$ .

4)         $\pi^i(s) \leftarrow \arg \max_a Q_{\theta}(s, a)$ .

**end**

**end**

**return**  $\pi^I$

**end**

---

that shows the usability of DOP in complex high-dimensional and multi-agent domains. In particular, we evaluate DOP against multiple algorithms over a set of 3 different tasks, as shown in Figure 3. Specifically, we run our experiments on three high-dimensional problems, where either a robot is hyper-redundant, or multiple robots are involved: (1) a *cooperative navigation* application, where three robots have to coordinate in order to find the minimum path to their respective targets in a simple environment; (2) a *fetching task*, where a 7-DOF robotic arm has to fetch an object while avoiding an obstacle in the environment; and (3) a *handover task* among a NAO (humanoid) robot and a human.

To report our results, we compare against DQN [11], TD-search [18] and both a *vanilla-UCT* and *random-UCT* implementations. We refer to *vanilla-UCT* as the standard UCT algorithm that, at each iteration, expands every possible action in  $A_j$ , for every agent  $j$ . *Random-UCT*, instead, is a naive algorithm where at each step of the Monte-Carlo search one action is randomly expanded. Moreover, in the *handover* (Figure 3(b)) scenario, we compare the performance

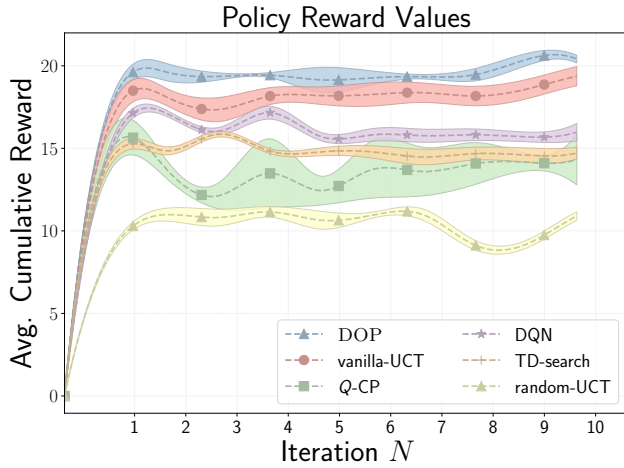
of DOP against the base  $Q$ -CP algorithm [12] and, we present the cumulative reward obtained by transferring the learned policy on a real NAO.

#### 4.1 Experimental Setup

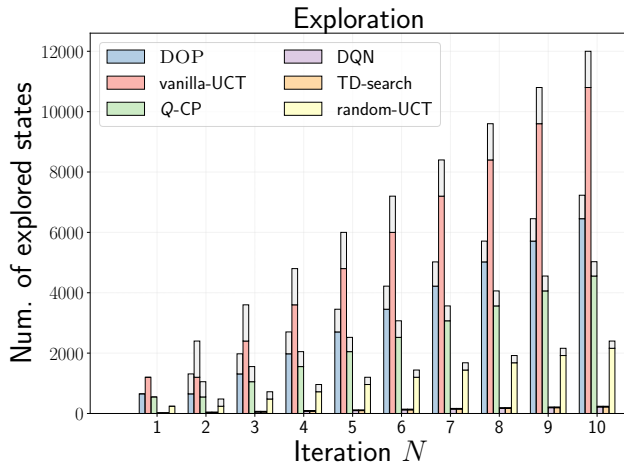
Experiments have been conducted using the V-REP simulator running on a single Intel Core i7-5700HQ core, with CPU@2.70GHz and 16GB of RAM. For all the scenarios, unless otherwise specified, the algorithm was configured with the same meta-parameters. The UCT horizon is set to  $H = 4$  to trade-off between usability and performance of the search algorithm; the number of roll-outs is set to be  $M = 3$ , while admissible actions are evaluated with an initial  $\lambda = 0.5$ , and  $\epsilon_{\hat{A}} = 0.3$ , guaranteeing good amounts of exploration. The  $C$  constant in Eq. 3 is set to 0.7. The learning rate  $\alpha$  is set to 0.15, while the discount factor  $\gamma$  is equal to 0.8. The state space, the set of actions and the reward functions are finally chosen and implemented depending on the robots and applications. In each of the proposed applications, stochastic actions are obtained by randomizing their outcomes with a 5% probability. We evaluate the cumulative reward obtained during different executions of DOP against the number of explored states and iterations of the algorithms. In our environments, we adopt a *shaped* reward function, thus providing a reward to the agent at each of the visited states.

#### 4.2 Cooperative Navigation

In this scenario, three robots have to perform a cooperative navigation task in a simple world composed by 16 reachable squares distributed on a 4x4 grid (see Figure 3(a)). The goal is assigned individually to each robot and consists in finding the minimum collision-free path to target square matching the their color (highlighted in the figure). The state is represented through an image collected from the top by an overlooking camera (i.e., all the robots are visible), while the set of discrete actions is composed by  $A = \langle \text{noop}, \text{up}, \text{down}, \text{right}, \text{left} \rangle$ . The reward function is normalized between  $[0, 1]$  and is shaped to be inversely proportional to the sum of the minimum path steps from the robot positions and targets. Figure 4 shows the results obtained by DOP against  $Q$ -CP [12], TD-search, DQN, *random-UCT* and *vanilla-UCT*. Figure 4(a) reports the average cumulative reward and standard deviation (line width) over



(a) Rewards



(b) States

**Figure 4: Average cumulative reward (a) and number of explored states (b) obtained by DOP, DQN, TD-search, *random-UCT* and *vanilla-UCT* in 10 iterations in the cooperative navigation scenario. For each of them, the cumulative reward is averaged over 10 runs. The averaged reward is represented as a dotted line while, the line width represent its standard deviation. At each iteration, the number of explored states is represented as a bar, where the height indicates the total number of visited states, and the top gray bar highlights the amount of states added during the particular iteration  $i$ .**

10 iterations – averaged over 10 runs – for each of the implemented algorithms. Figure 4(b), reports the number of states explored per iteration. Bars represent the number of states explored until the  $i$ th iteration, and the top gray bar highlights the amount of states expanded during iteration  $i$  against the number of states explored until  $i - 1$ . The results show different behaviors for each of the algorithm: *random-UCT* reports a low number of explored states – since

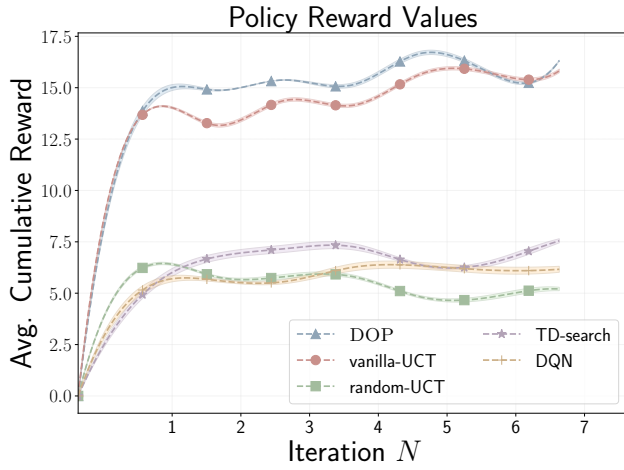
it only expands one random action at each UCT iteration – but, as expected, it performs poorly. Similarly, TD-search and DQN show a good trade-off between number explored states and cumulative reward, however, they are not able to generate competitive policies with few iterations and a reduced number of training samples. On the other hand, if we consider *vanilla-UCT* and DOP the algorithms report comparable cumulative rewards. However, our algorithm is able to generate a competitive policy with a reduced number of explored states – typically half the number of *vanilla-UCT* (~45% lower). *Q-CP* obtains a lower cumulative reward while visiting a slightly reduced number of states with respect to DOP. In fact, its reduced representational power does not enable the algorithm to immediately generalize informative states that need to be explored to obtain a better policy. Finally, it is worth highlighting that, even if both DQN and TD-search present a good trade-off between number of explored states and performance, they are not able to complete the task since initial iterations.

### 4.3 Fetching Task

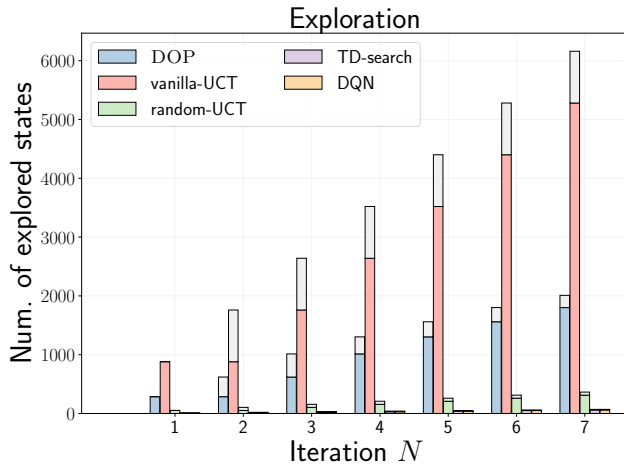
Here, the 7-DOF KUKA lightweight arm has to learn to fetch an object (e.g. a glass, Figure 3(c)) while avoiding an obstacle (a plant). In this scenario, the state space is again represented through an image collected by an overlooking camera, and the discretization of the state space is realized as described in Section 3.2. The robot can perform 10 actions:  $A = \langle \text{arm-up, arm-down, arm-forward, arm-backward, arm-right, arm-left, pitch-turn-left, pitch-turn-right, yaw-turn-left, yaw-turn-right} \rangle$ . Rotations on the roll angle have been removed as they do not influence the desired orientation of the fetched object. The reward function is in  $[0, 1]$  and it is computed as a weighted sum of four components: the first is inversely proportional to the Euclidean distance of the end-effector to the target, the second it proportional to the distance to the virtual center of the obstacle, the third and the fourth are inversely proportional to the pitch and yaw angle respectively. In this way the reward function promotes states that are near the target, far from the obstacle, and with the end-effector oriented upwards. This is implemented to succeed in the fetching task of objects that are to be carried with a preferred orientation (e.g. a glass full of water). As for the cooperative navigation scenario, Figure 5 shows the performance of DOP, DQN, TD-search, *random-UCT* and *vanilla-UCT*. This scenario is key to highlight that our contribution is more suitable and practical in robotic tasks with large state space. In fact, since first iterations and with a reduced set of training samples, DOP is able to outperform other algorithms that need a huge training set to learn competitive policies, e.g. DQN. Still, *vanilla-UCT* shows comparable rewards, but the number of explored states for this algorithm is ~65% larger than DOP.

### 4.4 Human-Robot Handover

The last scenario is characterized by two agents performing a human-robot interaction. The robot has to complete an handover by receiving an object which is hold by a human. In this setting, the state is represented through the images collected by the cameras of the robot. Moreover, the agent can perform a set of 25 actions:  $A = \langle \text{body-noop, body-forward, body-backward, body-turn-left, body-turn-right, head-up, head-down, head-right, head-left,}$



(a) Rewards

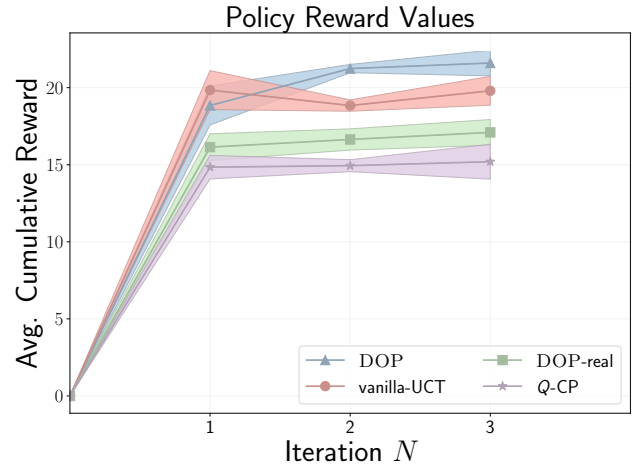


(b) States

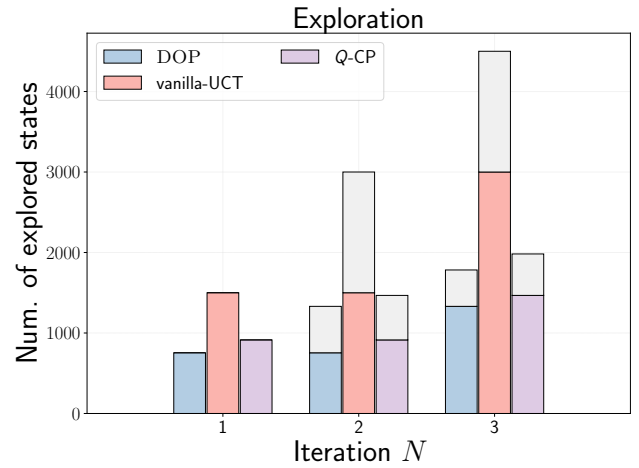
**Figure 5: Average cumulative reward and number of explored states obtained by DOP, DQN, TD-search, *random-UCT* and *vanilla-UCT* in 7 iterations in the Kuka fetching scenario. For each of them, the reward is averaged over 10 runs.**

right-arm-up, right-arm-down, right-arm-left, right-arm-right, right-arm-forward, right-arm-backward, left-arm-up, left-arm-down, left-arm-left, left-arm-right, left-arm-forward, left-arm-backward, open-right-hand, open-left-hand, close-right-hand, close-left-hand).

The (shaped) reward function is in  $[0, 1]$  and it is implemented as a weighted sum of 6 components: the first component is inversely proportional to the distance between the robot and the handed object, the second and third are inversely proportional to the distance from the object to the left and right hand respectively, the fourth component is inversely proportional to the distance between the ball and the center of the robot camera computed directly in the image frame, and the fifth and sixth components model the desired



(a) Rewards



(b) States

**Figure 6: Average cumulative reward and number of explored states obtained by DOP, *vanilla-UCT* and *Q-CP* in 3 iterations in the handover scenario. DOP-real reports reward values by transferring the DOP learned policy on a real robot. For each of them, the reward is averaged over 10 runs.**

status of the hands, promoting states that with open hands near the handed object. For this task, we choose a learning rate  $\alpha = 0.2$ .

The purpose of this experimental evaluation is to highlight both the quality of the learned policy when transferred in a real setting and the improvements of our representation with respect to *Q-CP*. Hence, we compare the results obtained by DOP against *Q-CP* and *vanilla-UCT*. As in previous scenarios, the two plots represent the obtained cumulative average reward and the number of explored states (Figure 6). As expected, DOP preserves the same improvements over the *vanilla-UCT* and, also in this case, our algorithm generates an effective policy with a remarkably reduced number of training examples. Differently, when comparing DOP against *Q-CP* we notice a similar number of explored states while DOP obtains

higher cumulative rewards. This shows the improved generalization capabilities of our representation, that is able to significantly improve performance while preserving sample complexity of the original algorithm. Finally, DOP-real shows the rewards obtained by transferring and rolling out the policy in real settings. In this case, the reward values show that, even though the robot does not perform as well as in simulation, it is still able to complete the task being robust to the noise of the real-world deployment. In fact, we consider the reduced cumulative reward values to be mostly due to noise in both the perception pipeline and motor encoders of the real NAO robot.

## 5 CONCLUSION

In this paper we introduced DOP, an iterative algorithm that uses action values learned through a deep  $Q$ -network to guide and reduce the exploration of the state space in different high-dimensional scenarios. Our key contribution consists in an extension of  $Q$ -CP [12] to use deep learning and improve both the focused exploration and the generalization of the algorithm. Thanks to the better generalization capabilities, DOP can be used in domains with high-dimensional states, such as multi-agent scenarios. For this reason, we evaluated both the representation and the algorithm on three different tasks that involve multiple or hyper-redundant robots. To better analyze the quality of the adopted representation, we also transferred a learned policy from simulation to real-world.

Unfortunately, DOP still needs a predefined simulation environment. This is not always available, and does not properly capture the dynamics of the world, making our algorithm less appealing in highly interactive scenarios. To address this issue, we aim at learning the dynamics of the world at robot operation time, and simultaneously improving its policy based on the learned model [21].

## REFERENCES

- [1] Cameron B Browne, Edward Powley, Daniel Whitehouse, Simon M Lucas, Peter I Cowling, Philipp Rohlfshagen, Stephen Tavener, Diego Perez, Spyridon Samothrakis, and Simon Colton. 2012. A survey of monte carlo tree search methods. *IEEE Transactions on Computational Intelligence and AI in Games* 4, 1 (2012), 1–43.
- [2] S. Calinon, F. D’halluin, E. L. Sauser, D. G. Caldwell, and A. G. Billard. 2010. Learning and Reproduction of Gestures by Imitation. *IEEE Robotics Automation Magazine* 17, 2 (June 2010), 44–54. <https://doi.org/10.1109/MRA.2010.936947>
- [3] Sylvain Gelly and David Silver. 2011. Monte-Carlo Tree Search and Rapid Action Value Estimation in Computer Go. *Artif. Intell.* 175, 11 (July 2011), 1856–1875. <https://doi.org/10.1016/j.artint.2011.03.007>
- [4] Steven James, George Konidaris, and Benjamin Rosman. 2017. An Analysis of Monte Carlo Tree Search.. In *AAAI*. 3576–3582.
- [5] Diederik P. Kingma and Jimmy Ba. 2014. Adam: A Method for Stochastic Optimization. *CoRR* abs/1412.6980 (2014). [arXiv:1412.6980](http://arxiv.org/abs/1412.6980) <http://arxiv.org/abs/1412.6980>
- [6] Levente Kocsis and Csaba Szepesvári. 2006. Bandit based monte-carlo planning. *Machine learning: ECML 2006* (2006), 282–293.
- [7] Sergey Levine, Chelsea Finn, Trevor Darrell, and Pieter Abbeel. 2016. End-to-end training of deep visuomotor policies. *Journal of Machine Learning Research* 17, 39 (2016), 1–40.
- [8] Sergey Levine, Peter Pastor, Alex Krizhevsky, Julian Ibarz, and Deirdre Quillen. 2016. Learning hand-eye coordination for robotic grasping with deep learning and large-scale data collection. *The International Journal of Robotics Research* (2016), 0278364917710318.
- [9] Timothy P Lillicrap, Jonathan J Hunt, Alexander Pritzel, Nicolas Heess, Tom Erez, Yuval Tassa, David Silver, and Daan Wierstra. 2015. Continuous control with deep reinforcement learning. *arXiv preprint arXiv:1509.02971* (2015).
- [10] Volodymyr Mnih, Adria Puigdomenech Badia, Mehdi Mirza, Alex Graves, Timothy Lillicrap, Tim Harley, David Silver, and Koray Kavukcuoglu. 2016. Asynchronous methods for deep reinforcement learning. In *International Conference on Machine Learning*. 1928–1937.
- [11] Volodymyr Mnih, Koray Kavukcuoglu, David Silver, Andrei A. Rusu, Joel Veness, Marc G. Bellemare, Alex Graves, Martin Riedmiller, Andreas K. Fidjeland, Georg Ostrovski, Stig Petersen, Charles Beattie, Amir Sadik, Ioannis Antonoglou, Helen King, Dhharshan Kumaran, Daan Wierstra, Shane Legg, and Demis Hassabis. 2015. Human-level control through deep reinforcement learning. *Nature* 518, 7540 (26 02 2015), 529–533. <http://dx.doi.org/10.1038/nature14236>
- [12] Francesco Riccio, Roberto Capobianco, and Daniele Nardi. 2018. Q-CP: Learning Action Values for Cooperative Planning. In *2018 IEEE International Conference on Robotics and Automation (ICRA)* (2018-01-30). –.
- [13] Stéphane Ross and J Andrew Bagnell. 2014. Reinforcement and imitation learning via interactive no-regret learning. *arXiv preprint arXiv:1406.5979* (2014).
- [14] Stéphane Ross, Geoffrey J Gordon, and Drew Bagnell. 2011. A Reduction of Imitation Learning and Structured Prediction to No-Regret Online Learning. In *International Conference on Artificial Intelligence and Statistics*. 627–635.
- [15] Andrei A Rusu, Matej Vecerik, Thomas Rothörl, Nicolas Heess, Razvan Pascanu, and Raia Hadsell. 2016. Sim-to-real robot learning from pixels with progressive nets. *arXiv preprint arXiv:1610.04286* (2016).
- [16] David Silver, Aja Huang, Chris J Maddison, Arthur Guez, Laurent Sifre, George Van Den Driessche, Julian Schrittwieser, Ioannis Antonoglou, Veda Panneershelvam, Marc Lanctot, et al. 2016. Mastering the game of Go with deep neural networks and tree search. *Nature* 529, 7578 (2016), 484–489.
- [17] David Silver, Julian Schrittwieser, Karen Simonyan, Ioannis Antonoglou, Aja Huang, Arthur Guez, Thomas Hubert, Lucas Baker, Matthew Lai, Adrian Bolton, et al. 2017. Mastering the game of go without human knowledge. *Nature* 550, 7676 (2017), 354–359.
- [18] David Silver, Richard S Sutton, and Martin Müller. 2012. Temporal-difference search in computer Go. *Machine learning* 87, 2 (2012), 183–219.
- [19] Wen Sun, Arun Venkatraman, Geoffrey J. Gordon, Byron Boots, and J. Andrew Bagnell. 2017. Deeply AggreVaTeD: Differentiable Imitation Learning for Sequential Prediction. In *Proceedings of the 2017 International Conference on Machine Learning (ICML)*.
- [20] Matej Večerik, Todd Hester, Jonathan Scholz, Fumin Wang, Olivier Pietquin, Bilal Piot, Nicolas Heess, Thomas Rothörl, Thomas Lampe, and Martin Riedmiller. 2017. Leveraging demonstrations for deep reinforcement learning on robotics problems with sparse rewards. *arXiv preprint arXiv:1707.08817* (2017).
- [21] Théophane Weber, Sébastien Racanière, David P Reichert, Lars Buesing, Arthur Guez, Danilo Jimenez Rezende, Adria Puigdomènech Badia, Oriol Vinyals, Nicolas Heess, Yujia Li, et al. 2017. Imagination-augmented agents for deep reinforcement learning. *arXiv preprint arXiv:1707.06203* (2017).
- [22] Mark H. Winands, Yngvi Björnsson, and Jahn-Takeshi Saito. 2008. Monte-Carlo Tree Search Solver. In *Proceedings of the 6th International Conference on Computers and Games (CG ’08)*. Springer-Verlag, Berlin, Heidelberg, 25–36. [https://doi.org/10.1007/978-3-540-87608-3\\_3](https://doi.org/10.1007/978-3-540-87608-3_3)